REFERENCES

1. Gavrilov V.V. Methods of improving carburetion and combustion in marine diesel on the basis of mathematical and physical modeling of local intracylinder processes: Abstract of a thesis ... of doctor of tech. science. – St.-Petersburg: SPSMTU, 2004. – 43 p.
2. Diesel engine operation in under field conditions / A.K. Kostin, B.P. Pugachev, Yu.Yu. Kochenev; ed. by A.K. Kostin. – Leningrad: Mashinostroenie, 1989. – 284 p.
3. Schukin P.A. Complex mathematical model of operation of diesel engine with volumetric carburetion. Abstract of a thesis ... of a cand. of tech. science. – St.-Petersburg: TsNIDI, 1999. – 22 p.

Received on 15.01.2007

UDC 620.18:669.14

THIN STRUCTURE OF STEEL St52,3N AND POSSIBLE REASONS OF DEFECT OF LARGE-CAPACITY BILLETS AT «YURMASH»

V.I. Danilov*, D.V. Valuev, Yu.F. Ivanov**, A.M. Apasov

Technological institute, TPU branch, Yurga
E-mail: mchmyti@rambler.ru
*Institute of physics of strength and material science of RAS SD, Tomsk
**Institute of high-current electronics of RAS SD, Tomsk
E-mail: dvi@ispms.tsc.ru

Electron-microscopic and x-ray investigations of structurally-phase and intense-deformed condition of material made of defective and conditional forged billet at «Yurmash» have been carried out. It is ascertained that in steel made from the defective forged piece the fraction of perlite is 1,5...2 times higher and lamellar perlite prevails. Local long-range tensions in both conditions of material are commensurable with fluidity limit. The content of sulfides is considerably higher in the steel made from the defective billet. They are located in the body of ferrite grains and along the interfaces. In the material made from the conditional forging they are located only inside of grains. The scalar density of dislocations in ferrite grains and in ferrite layers of perlite of the defected billet is one and a half time higher than in conditional metal. All the totality of the listed above circumstances allows stating that the main cause of cracking of large-capacity billets made of steel St52,3N is not a full conformity of the chemical compound to branded requirements.

1. Introduction and prestarting procedures

In the article [1] the following conclusion was drawn – it is impossible to determine the reasons of cracking the forgings of steel St52,3N without estimation of mode of deformation, precision investigations of structure, the analysis of defective subsystem state and ascertainment of crystal-chemical nature of secondary phase precipitations. Really, optical microscopy does not allow even determining precisely the perlite morphology, although, granular perlit is more preferable than lamellar one in critical product [2]. The most important factor determining article structural strength are the internal residual stresses [3] which are not metallographically controlled at all. Besides, secondary phase precipitations are qualified in steels by metallographic technique only as nonmetallic inclusions of proper point [4], however, carbide, oxide, sulfide and phosphide phases influence differently the operating characteristics. All the listed problems may be solved by the methods of X-ray diffraction analysis and transmission electron microscopy.

In this work the electron microscopic investigations were carried out at transmission microscope UEMV-125K in light and dark fields. Electron diffraction patterns of reflexes in dark field were recorded for analyzing crystal structure of secondary phases. Foils for researches were cut by electric-spark method from samples which were used before in metallographic analysis. Final preparations of foils were carried out by electropolishing. Thin structure of steel made of defective and conditioned forging was studied. A type of dislocation substructure in ferrite grains and perlite ferrite layers, perlite colony structure, shape, sizes, position and composition of secondary phase particles, level of internal long-range stresses were determined.

2. The results of electron microscopy of defective forging material

An attempt to use the X-ray diffraction analysis for identifying secondary phases and estimating internal stresses turned out to be unsuccessful. It is, probably, connected with the fact that sulfide, phosphide and oxide phases present in steel in mass concentrations lower than the detection limit by the X-ray method. Carbide phase is presented by cementite which is not roentgenographically detected at α-Fe. Internal stresses of the I kind may be defined only in the whole article and the stresses of the II kind turned out to be lower than the level of reliable identification both in defective and conditioned metal. One succeeded in ascertaining that lattice parameter of defective forging metal is higher, that indicates the increased content of interstitial impurities – carbon, first of all. Therefore, the main attention was given to electron microscopic investigations.

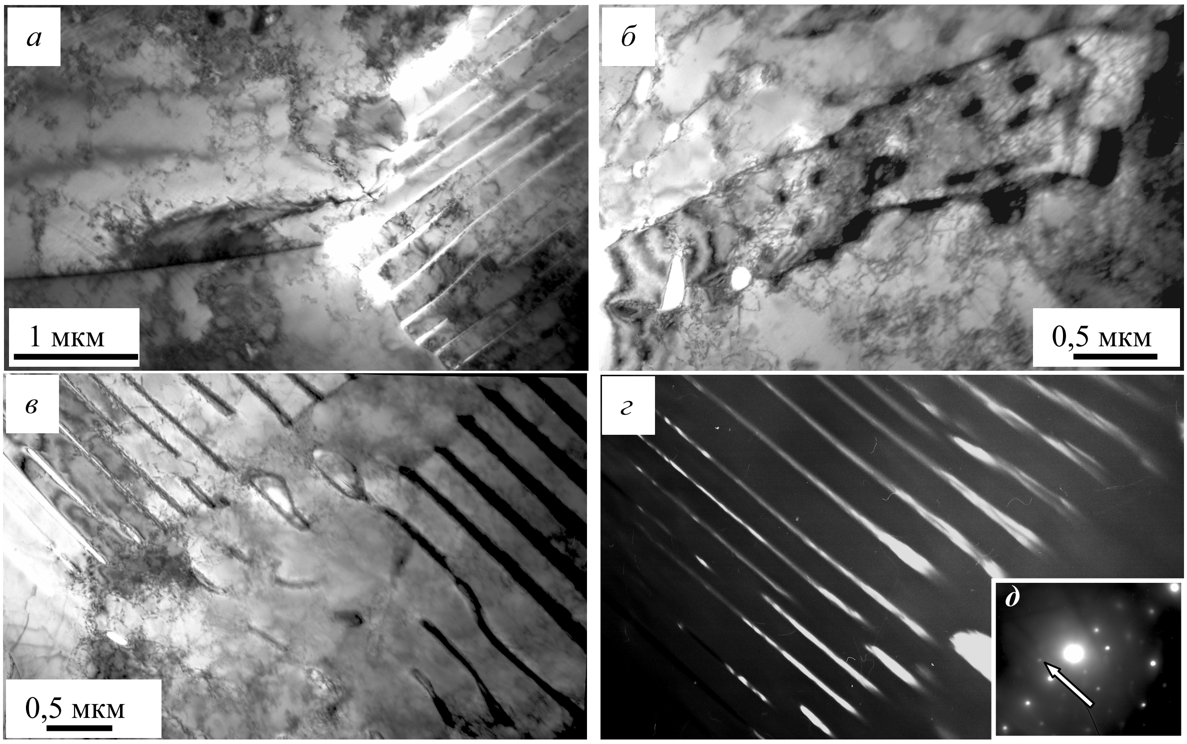

Fig. 1. *Electron microscopic images of steel St52,3N structure, made of defective forging. a–c) light field images; d) dark field obtained in reflex [130]Fe$_3$C; e) micro-electron diffraction pattern to (c), dark field reflex is indicated by an arrow*

The results of transmission electron microscopy confirmed that the material of defective billet is a polycrystalline aggregate consisting of ferrite grains and perlite colonies. Typical electron microscopic image of ferrite, perlite of globular and lamellar morphology is given in Fig. 1, *a*, *b*, *c*, respectively. In most cases the perlite colonies are located in ferrite grain boundary junctions or they are extended along these boundaries dividing adjacent ferrite grain as, for example, globular perlite colony in Fig. 1, *b*. In total compliance with optical microscopy data, perlite lamellar morphology is predominant. Typical feature of lamellar perlite colonies is a high level of cementite plates imperfection which are greatly curved, contain ferrite bridges and their lateral dimensions change by plate length (Fig. 1, *c*, and Fig. 2).

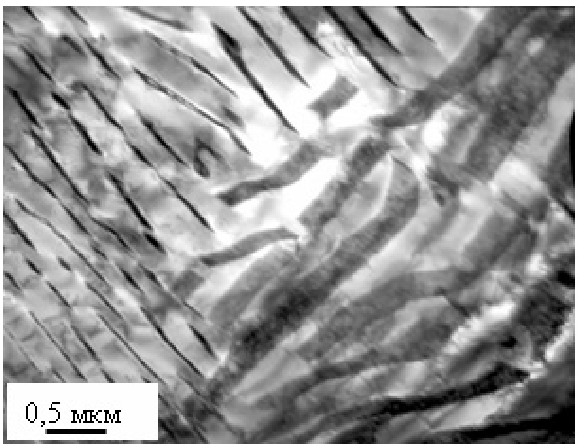

Fig. 2. *Electron microscopic image of the structure of lamellar perlite of steel St52,3N of defective forging*

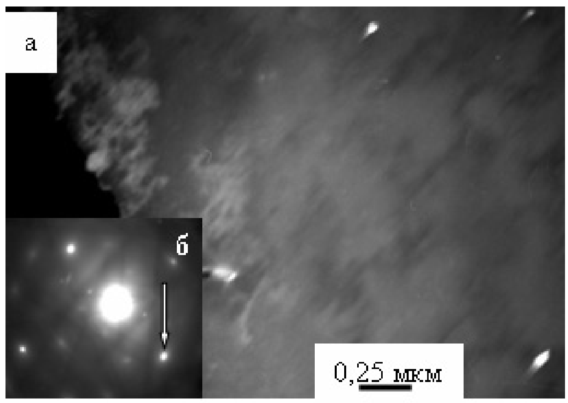

Fig. 3. *Electron microscopic image of the structure of steel St52,3N of defective forging; a) dark field obtained in reflex [200] FeS$_2$; b) micro-electron diffraction pattern to (a). Dark field reflex is indicated by an arrow.*

A type of dislocation substructure was determined separately in ferrite grains and perlite ferrite plates. It is turned out that perlite ferrite plates show higher level of imperfection. In ferrite grains the ball and net substructures are recorded and dislocation scalar density amounts to ~$2{,}6\cdot10^{10}$ см$^{-2}$ (Fig. 1, *a*), in perlite ferrite plates only net dislocation substructure is observed at scalar density $3\cdot10^{10}$ см$^{-2}$ (Fig. 1, *c*, and Fig. 2).

The second phase particles are recorded in a body of ferrite grains and perlite ferrite plates, along the boundaries and in triple junction. If the particles are located in grain volume then they always have round, globular shape (Fig. 3). Average sizes of such particles amount to ~13 nm. Microdiffraction electron microscopic analysis

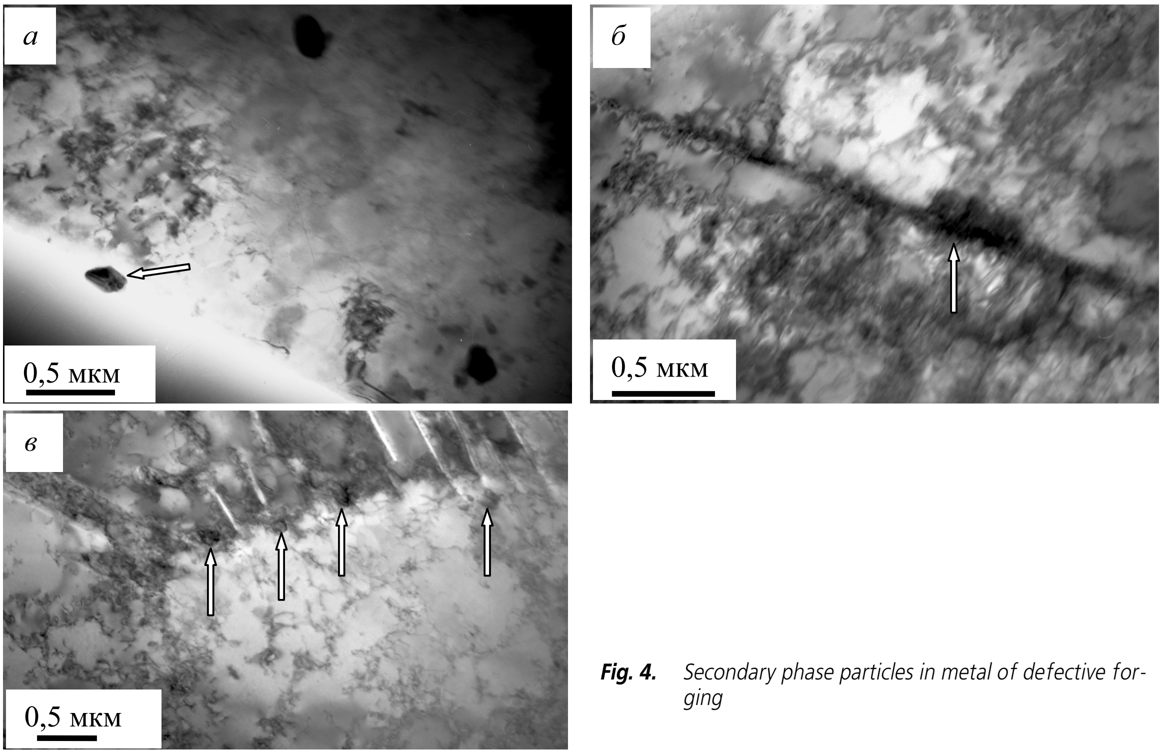

Fig. 4. *Secondary phase particles in metal of defective forging*

shows that these particles are iron sulfide of compositions FeS or FeS_2. Particles situated along grain boundaries are divided into three morphological varieties: particles with crystal faceting (Fig. 4, *a*), and thin layers (Fig. 4, *b*) and globules (Fig. 4, *c*). In ferrite grain boundary junctions the second phase particles have almost everywhere globular shape. Microdiffraction analysis shows that globular morphology particles represent ferric carbide of cementite type regardless of place of their arrangement. Particles in the form of thin layers have more complex chemical composition. They may be iron sulfides or chromium sulfides of the type MeS. Besides, faceting shape particles are always iron sulfides FeS.

Relatively high content of perlite in steel St52,3N of defective forging attracts attention. According to the frequency of perlite colony encounters, in foils carbon concentration in material should be on the level not lower than ~0,3 wt. %. This feature coordinates well with optical microscopy data and does not contradict the results of X-ray diffraction analysis.

The important feature of electron microscopic images of steel structural constituents of defective forging is presence of bend extinction contours in them which reflect bending-rotating of crystal lattice. Bending-rotating sources are interfaces (Fig. 1, *a*) or chains of the secondary phase particles (Fig. 4, *b*, *c*). The method of determining the value of internal long-range stresses is described by geometrical parameters (width) of bend extinction contours [5]. It is seen (Fig. 4, *b*) that the narrowest extinction contours are observed along the chains of sulfide inclusions. Here, internal long-range stresses may achieve 300...350 MPa that is comparable and even exceeds steel yield strength [1]. Authors [5] indicate that the long-range stresses determined by electron microscopic method reflect material state in microvolumes, therefore, as a rule, they are rather higher of an average level which is estimated by roentgenographic method. But these very stresses control the processes of plastic flow and collapse on microlevel.

3. The results of electron microscopy of conditioned forging material

Electron microscopic investigations of steel St52,3N of conditioned forging showed that its structure differs considerably from metal structure of defective billet at general qualitative similarity. Material is also a ferrite-perlite aggregate (Fig. 5) but perlite quantity is lower and corresponds to carbon mark content on the level 0,2 wt. %. Besides, grain perlite (Fig. 5, *c*) is a dominant one, but not lamellar perlite (Fig. 5, *b*). In most cases perlite colonies are located in ferrite grain boundary junctions or they are expanded along ferrite grain boundaries dividing them. Colonies of scarce lamellar perlite have a high level of cementite plate imperfection as well – plates are curved, contain ferrite gaps; plate lateral dimensions change randomly along the plate length. Dislocation substructure in ferrite grain volumes is also net or ball (Fig. 5, *a*) but dislocation scalar density is rather lower than in defective billet and amounts to $\sim 2{,}3\cdot 10^{10}$ cm^{-2}. In perlite ferrite plates the substructure of dislocation chaos or net dislocation substructure are observed (Fig. 5, *b*). Dislocation scalar density in them is lower – $1{,}8\cdot 10^{10}$ cm^{-2}; at the same time, in defective forging the ratio of dislocation densities in ferrite and perlite was opposite.

In the volume and on ferrite grain boundaries the second phase particles are observed. The particles located in grain volume have round shape, their average sizes

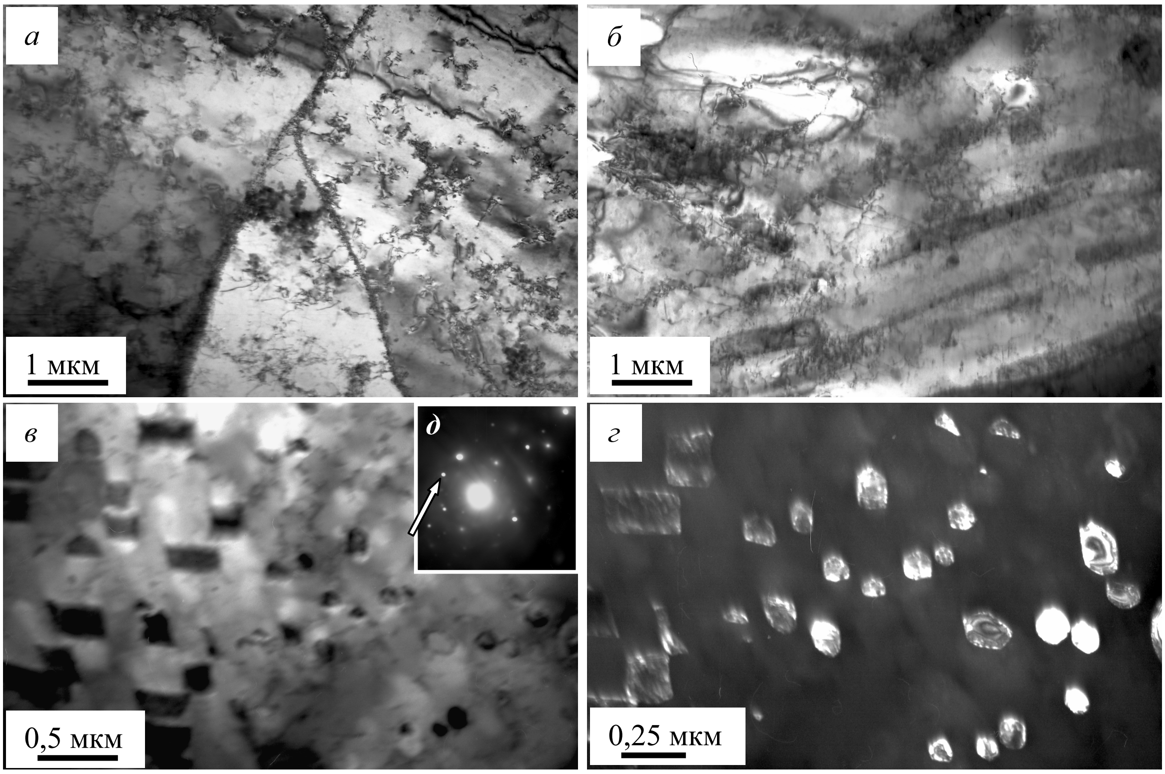

Fig. 5. *Electron microscopic images of the structure of steel St 52,3N of conditioned forging; a–c) light field images; d) dark field obtained in reflex [031] Fe_3C; e – micro-electron diffraction pattern to (c), dark field reflex is noted by an arrow*

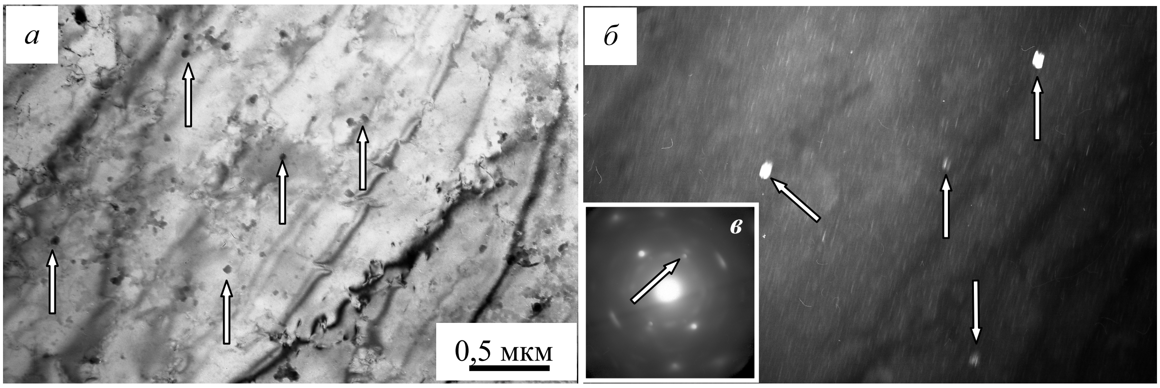

Fig. 6. *Electron microscopic images of the structure of steel St52,3N of conditioned forging; a) light field images; b) dark field obtained in reflex [101] FeS_2; c) micro-electron diffraction pattern to (a). In (a, b) – particles of iron sulfide; in (c) – dark field reflex are noted by arrows*

amount to ~43 nm (Fig. 6). Microdiffraction electron microscopic analysis shows that these formations are (in most cases) iron sulfides (Fig. 6, *c*). Particles along grain boundaries have two morphological varieties – globules (Fig. 7, *a*) and thin layers (Fig. 7, *b*); in ferrite grain boundary junctions the second phase particles have almost always globular shape (Fig. 7, *a*).

Microdiffraction analysis shows that globular morphology particles are the iron carbide – cementite, regardless to their arrangement. Particles in the form of thin layers have more complex chemical composition. These layers are often formed by iron carbide of composition Fe_3C, seldom by -silicon carbide of composition SiC. It should be noted that the second phase in the form of thin layers along grain boundaries is seldom observed and detected approximately in one case per thirty ferrite grain boundaries. Generally, the arrangement of the second phase precipitations along grain boundaries is not typical in material of conditioned forging.

Internal long-range stresses present in conditioned forging material as the bend extinction contours are observed on electron microscopic images. The latter are also often connected with the secondary phase chains (Fig. 6, *a*). According to the designs by the technique [5] the value of local long-range stresses differs slightly from the level of stresses in material of defective forging.

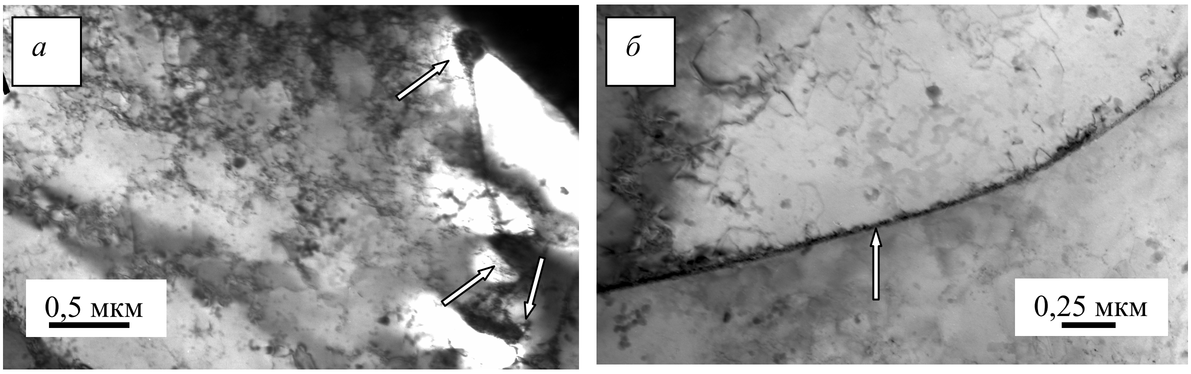

Fig. 7. *Particles of globular shape (a) in metal grain junctions of conditioned billets (noted by arrows) and particles of plastic form (b) in metal grain boundary of conditioned forging*

Discussion of the results and conclusions

X-ray diffraction analysis and electron microscopic investigations of the material of both defective and conditioned forging allowed ascertaining.

1. The analyzed steel samples are really polycrystalline aggregates formed by ferrite grains and perlite colonies. Perlite may be divided by morphological feature into lamellar and globular ones.
2. Perlite volume fractions of in steel of defective and conditioned forging differ considerably. In the first case the relative perlite volume fraction is in 1,5...2 times higher and it means that carbon concentration is increased relative to mark content, it may amount to ~0,3 wt. %. Lamellar perlite prevails by morphological feature in defective metal.
3. The level of internal stresses of the II kind in both forgings is on detection limit by X-ray diffractometer method. Local long-range stresses estimated by electron microscopic method are, on the contrary, high and comparable with yield point in both material states as well.
4. Dispersed carbides and inclusions of sulfide type located in the volume and along the boundaries of ferrite grain and perlite ferrite plates are observed in both states. Sulfide content is rather higher in the steel sample of defective billet; they are arranged in ferrite grain bodies and along the interfaces, while in the material of conditioned forging – only inside the grains.
5. At similar types of dislocation substructures (ballnet and net) the imperfection level in steel of defective forging is considerably higher than of conditioned article. Dislocation scalar density in ferrite grains and ferrite layers of defective billet amounts to $2{,}6\cdot10^{10}$ and $3\cdot10^{10}$ cm^{-2}, respectively, that is in 1,1...1,7 times higher than in conditioned metal.

If we generalize the results of mechanical tests, optical metallography [1] and electron microscopy then one can come to the definite conclusion – the reason of cracking large-capacity billets of steel St52,3N is not full is not a full conformity of the chemical compound to branded requirements. The increased content of carbon and, probably, sulfur turned out to be in defected forging. The first factor is confirmed both by the results of optical metallography and electron microscopy. The second factor is determined only as a result of diffraction electron microscopic investigations. The effect of the first factor was decrease of the temperature of critical point A_3, which may achieve 30...70 °C. For example, according to [6, 7] at carbon concentration ~0,2 wt. % and without other alloying A_3=860 °C, at carbon content ~0,3 wt. % A_3=830 °C. As a result, using standard technology, steel turns out to be overheated at warming for final thermal treatment. Besides, stability of overchilled austenite changes. More nonequilibrium structures with high level of imperfection and residual long-range stresses are formed at the same cooling rate in steel with increased carbon content. Austenite in such steel possesses the increased strength; therefore higher degrees of reduction at hot forming are required.

All the totality of the listed facts resulted in deficient deformation degree at forming that was stated in [1] by fracture analysis. Deficient deformation degree, in its turn, at hot forging conditioned the formation of a majority of pores and microcracks and relatively high temperature – output to the boundaries of interstitial impurities with formation of the secondary phases in the form of thin layers. The decrease of plasticity of defective forging material relative to ES requirements by stated in [1] is a direct effect of nonoptimal structure both on macroscopic and microscopic levels. The position is aggravated by the fact that sulfur content in defective metal turned out to be on the upper level of the acceptable one by grade composition. However, at standard carbon content, this circumstance does not result in critical effects.

REFERENCES

1. Apasov A.M., Valuev D.V., Danilov V.I. On possible reasons of defects of large-capacity billets of low-carbon manganese steel at «Yurmash» // Bulletin of the Tomsk Polytechnic University. – 2007. – V. 310. – № 3. – P. 90–92.
2. Tushinskiy L.I., Bataev A.A., Tikhomirova L.B. Perlite structure and constructive strength of steel. – Novosibirsk: Nauka, 1993. – 280 p.
3. Lyubimova L.L. The technique of roentgenometric analysis of instructure stresses // Bulletin of the Tomsk Polytechnic University. – 2003. – V. 306. – № 4. – P. 72–77.
4. Malinina R.I., Malyutina E.S., Novikov V.Yu. et al. Practical metallography. – Moscow: Intermet Engineering, 2004. – 230 p.
5. Structural-phase states of metal systems / Ed. by A.I. Potekaeva. – Tomsk: Press of NTL, 2004. – 356 p.
6. Metal research and steel thermal treatment. Reference book. V. II. The fundamentals of thermal treatment / Ed. by M.L. Bernshtein, A.G. Rathshtadt. – Moscow: Metallurgiya, 1995. – 336 p.
7. Sorokin V.G., Gervasiev M.A., Paeev V.S. et al. Steels and alloys. – Moscow: Intermet Engineering, 2001. – 608 p.

Received on 22.12.2006

UDC 621.313.12

COMPUTATION OF CURRENT PULSED SOURCES WITH INDUCTIVE ENERGY STORAGES

G.V. Nosov

Tomsk Polytechnic University
E-mail: nosov@elti.tpu.ru

Formulas for computation of efficiency and parameters of current pulsed sources at charging and discharging of the inductive energy storage on active loading have been obtained. For charging the inductive storage the electric and capacitor batteries, unipolar and synchronous electric generators with the rectifier, equivalent circuit of which can be presented by consecutive connection of equivalent capacity, inductance and resistance are considered. Formulas, at which high efficiency of charge is reached, are obtained for computation of parameters of the inductive storage in the form of the multilayered coil. It is shown that current pulsed sources are the most effective at oscillatory charging of the inductive storage when more than 50 % of the generator energy can be transferred to loading.

Currently, pulsed sources with resistive («hot») inductive storages of electromagnetic energy W and open (explosive) switches K_2 (Fig. 1) are one of the most powerful current pulse generators with specific accumulated energy in inductive storage to 5 J/g and more [1–3]. Therefore, computation of the efficiency and parameters of such source is the topical problem.

To charge the inductive storage with energy W let us examine such electromagnetic energy generators as accumulator and capacitor batteries charged from internal source as well as unipolar and synchronous electric generators with rectifier in electrodynamic braking mode [1–3].

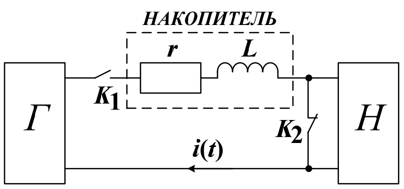

Fig. 1. *Diagram of charging inductive storage and pulse loading supply: Г is the electromagnetic energy generator; H is the loading; K_1 and K_2 are the switches; L and r are the inductance and resistance of storage wire*

The equivalent circuit of these generators may be approximately introduced in the form of series connection of capacity C_g, inductance L_g and resistance r_g [2, 3], then, for equivalent parameters of a circuit of inductive storage loading

$$C_g = \frac{2W_g}{U_g^2}; \quad r_z = r_g + r; \quad L_e = L_g + L, \qquad (1)$$

when switches K_1 and K_2 are closed, one determines the roots of characteristic equations

$$p_{1,2} = -\frac{r_z}{2L_e} \pm \sqrt{\frac{r_z^2}{4L_e^2} - \frac{1}{L_e C_g}} \qquad (2)$$

and charging time of inductive storage ($p_1 \neq p_2$)

$$t_z = \frac{\ln(p_2 / p_1)}{p_1 - p_2}, \qquad (3)$$

corresponding to current maximal value $i(t)$

$$I_m = i(t_z) = \frac{C_g U_g p_1 p_2}{p_1 - p_2}[e^{p_1 t_z} - e^{p_2 t_z}] \qquad (4)$$

and maximal energy accumulated by the storage

$$W = \frac{L I_m^2}{2} \qquad (5)$$

at voltage magnitude at capacitance C_g

$$U_z = u_C(t_z) = \frac{U_g p_2}{p_1 - p_2}\left[e^{p_1 t_z} - \frac{p_1}{p_2} e^{p_2 t_z}\right], \qquad (6)$$

where W_g and U_g are the initial values of accumulated energy and voltage of generator at open switch K_1, respectively (Fig. 1).